

Detecting $H \rightarrow hh$ in the Mirror Model at the CERN Large Hadron Collider

Wen-sheng Li, Peng-fei Yin and Shou-hua Zhu

Institute of Theoretical Physics, School of Physics, Peking University, Beijing 100871, China

(Dated: February 1, 2008)

The Higgs sector may play an important role in detecting the mirror particles, which can be the candidates of the dark matter and appear as missing energy in the detectors at the LHC. In this paper we worked out the Higgs boson spectrum and the Higgs couplings for the symmetric vacuum, namely $v_1 = v_2 = v$, in the mirror model, and investigated the constraints from electroweak precision observable (EWPO). Our study showed that the EWPO has already constrained the Higgs boson sector severely. We then explored the Higgs boson phenomenology, and focused on the scenario that the heavier Higgs boson H can decay into a pair of lighter Higgs boson h . We proposed to study the invisible decay of the Higgs boson via the pair production of them, in which one Higgs boson decays into bottom quarks and the other decays invisibly. Our detail simulation for signals and backgrounds showed that the observation of signal can reach 5σ significance for $m_H = 260$ GeV and $m_h = 115$ GeV with $10fb^{-1}$ integrated luminosity at the LHC. Moreover the possible method to further suppress dominant $Zb\bar{b}$ background was discussed. We also simulated the signals and backgrounds for $H \rightarrow hh \rightarrow 4b$. Our results showed that it is very difficult to isolate the signals from huge QCD continuum backgrounds.

PACS numbers: 12.60.Fr, 12.80.Bn, 14.80.Cp

I. INTRODUCTION

Why only the left-handed fermions can feel weak interaction, while the right-handed fermions can't, is a long-standing fundamental question in the standard model (SM) of particle physics. Basically speaking there are two category models to solve this issue. The first ones are the so-called left-right symmetric models, in which the $SU(2)$ singlet right-handed fermions in the SM are assumed to involve the new gauge interaction. Many models of this kind have been constructed based on the minimal gauge group $SU(2)_L \otimes SU(2)_R \otimes U(1)_{B-L}$ since the seventies in the last century [1, 2]. The second ones are mirror models, in which the usual SM fermions and/or gauge boson are accompanied by the mirror partners, similar to the case in the supersymmetric models. This idea was first proposed by Lee and Yang in 1956 [3]. Based on this naive conjecture, many models were constructed. An excellent extensive review on this subject can be found in Ref. [4]. One of the advantages of the left-right symmetric models is that parity can be restored at higher energy. However the parity restoration scale has been pushed higher and higher, namely up to several TeVs because of severe constraints from the precise measurements of the low energy experiments, for example from the measurement of $K_0 - \bar{K}_0$ mixing.

In this paper we will consider the mirror models. Besides providing a way to understand parity restoration, the mirror particles in the mirror models can provide *natural* candidates for the dark matter. It is well known that the SM can provide an excellent description for particle experiments at energies so far probed. But it can not give any explanation for dark matter. Thus people expect that new physics beyond the SM can provide a natural candidate for the dark matter. At present, the most popular candidate for the (thermal-produced)

dark matter is the so-called weakly-interacting-massive-particle (WIMP). There are some popular candidates for WIMPs, for example lightest supersymmetric particle (LSP), axion and lightest Kaluza-Klein particle (LKP) in universal extra dimension models etc. However the new observations of dwarf spheroidal galaxies seem indicate that non-cold dark matter (e.g. sterile neutrino) needs to be considered seriously [5]. Mirror models [6] can also give this kind of candidate for dark matter.

Besides the cosmological evidences, we need also inputs from collider experiments, for example the Large Hadron Collider (LHC) and International Linear Collider (ILC), in order to reach the decisive conclusions on the properties of dark matter. The basic assumption here is that the dark matter should couple to usual SM matter. In mirror models mirror particles can couple to ordinary particles through three kinds of renormalizable gauge invariant interactions. The first possibility is through neutrino mixing if the SM right-handed neutrino, as well as the corresponding mirror fields, are introduced. If neutrinos have masses, then the mixing between ordinary and mirror neutrinos is possible. The discussion of this possibility can be found in Ref. [7]. The other two possibilities are 'kinetic mixing' and 'scalar mixing', expressed as

$$L_{mix} = \epsilon F^{\mu\nu} F'_{\mu\nu} + \eta \phi_1^\dagger \phi_1 \phi_2^\dagger \phi_2 \quad (1)$$

with F' and ϕ_2 the mirror fields of usual $U(1)$ gauge and Higgs fields respectively in the SM. In Eq. 1, $F^{\mu\nu} F'_{\mu\nu}$ will give electric charge to mirror quarks and leptons. Because QED has been tested very precisely, the mixing parameter ϵ is severely constrained to be extremely small [8, 9, 10], which should play a negligible role at LHC and ILC. The same conclusion applies also to the neutrino mixing case. Thus in this paper we will concentrate on the third possibility: scalar mixing.

As indicated in Eq. 1, mirror Higgs ϕ_2 can couple to ordinary SM Higgs ϕ_1 through renormalizable gauge invariant term $\eta\phi_1^\dagger\phi_1\phi_2^\dagger\phi_2$ with η the dimensionless free parameter. After electroweak symmetry spontaneously breaking, there remain two physical Higgs bosons. Each Higgs boson is the mixture state of SM and mirror Higgs fields. As a consequence, each Higgs boson will couple to both usual SM and mirror particles. So our primary interest in this paper is to investigate the mirror particle effects on the Higgs sector. The generic feature of Higgs boson is that Higgs boson can decay invisibly, i.e. into mirror particles. Such invisible decay can be searched in all production modes [12, 13], and the promising ones are associated production with Z boson $q\bar{q} \rightarrow HZ$, or through gauge boson fusion processes $VV \rightarrow H$, as well as associated production with top quark pairs etc.

In this paper we will focus on a new mode to search for the Higgs boson invisible decay at LHC, i.e. $gg \rightarrow H \rightarrow hh \rightarrow b\bar{b} + \text{mirror particles}$. Here H and h are the heavier and lighter Higgs boson in mirror model (see section II). The mirror particles will appear as the missing energy in the detectors. The advantage of this process is that light H can be produced copiously due to the gluon-gluon high luminosity. It is obvious that m_H is required to be larger than $2m_h$ in order to obtain large production rate. As shown below (section III), $m_H > 2m_h$ is allowed in the mirror model after imposing the constraints from electro-weak precision observable. In the mirror model, the coupling strength of H-h-h is proportional to $m_H^2 + 2m_h^2$ (section II), and the partial decay width of the mode $H \rightarrow hh$ can be even larger than those that into gauge bosons. Thus this process can be a promising channel to study the mirror model. In this paper we will also study the signals and backgrounds for the process $gg \rightarrow H \rightarrow hh \rightarrow b\bar{b} + b\bar{b}$. Our study shows that it is a **challenge** to observe this process due to the huge QCD backgrounds.

The paper is organized as following. In section II we briefly describe the mirror model, and work out the Higgs boson spectrum and interactions. In section III we investigate the constraints from electro-weak precision observables utilizing the S, T parametrization. In section IV we show the main results for the Higgs boson decays and main production channels. Section V contains the detail simulation for the signals and backgrounds for the process $gg \rightarrow H \rightarrow hh \rightarrow b\bar{b} + \text{mirror particles}$ and $gg \rightarrow H \rightarrow hh \rightarrow b\bar{b} + b\bar{b}$. The last section is allocated to discussions and conclusions.

II. MIRROR MODEL

In this section we briefly describe the mirror model (for full details to see Ref. [14]). In the quantum field theory, the usual parity translation takes \vec{r} to $-\vec{r}$ and t to t . In the left-right symmetric models parity is extended to a new type Z_2 discrete symmetry which transforms the left-handed field to the right-handed one for

the *same* fermion. Besides fermion sector, under such Z_2 the SM $SU(2)_L$ weak gauge boson fields transform to the new $SU(2)_R$ gauge bosons and vice versa. However such discrete symmetry is not solely fixed. Under Z_2 , the left-handed sector of fermion field can transform to the right-handed sector of *different* fermion field, namely the mirror fermion field. Based on this observation, one can extend the SM by doubling the ordinary fermion, gauge and Higgs fields [14]. Thus the new mirror fermions are natural singlets of the SM gauge group, and they (nucleus if there exists mirror $SU(3)_C$) can be the candidates for the dark matter. The minimal gauge group of the new mirror model is $G_{SM} \otimes G' = SU(3) \otimes SU(2) \otimes U(1) \otimes SU(3)' \otimes SU(2)' \otimes U(1)'$. The gauge quantum numbers under $G_{SM} \otimes G'$ for the usual and mirror fermion fields are

$$\begin{aligned} L_L^i &\sim (1, 2, -1)(1, 1, 0) \quad , \quad (L_R')^i \sim (1, 1, 0)(1, 2, -1) \\ e_R^i &\sim (1, 1, -2)(1, 1, 0) \quad , \quad (e_L')^i \sim (1, 1, 0)(1, 1, -2) \\ Q_L^i &\sim (3, 2, \frac{1}{3})(1, 1, 0) \quad , \quad (q_R')^i \sim (1, 1, 0)(3, 2, \frac{1}{3}) \\ u_R^i &\sim (3, 1, \frac{4}{3})(1, 1, 0) \quad , \quad (u_L')^i \sim (1, 1, 0)(3, 1, \frac{4}{3}) \\ d_R^i &\sim (3, 1, -\frac{2}{3})(1, 1, 0) \quad , \quad (d_L')^i \sim (1, 1, 0)(3, 1, -\frac{2}{3}) \end{aligned}$$

with i the family index.

The Z_2 parity symmetry that we define now is

$$\begin{aligned} \vec{r} &\leftrightarrow -\vec{r}, t \leftrightarrow t, \quad G^\mu \leftrightarrow G'_\mu, \quad W^\mu \leftrightarrow W'_\mu, \quad B^\mu \leftrightarrow B'_\mu \\ L_L &\leftrightarrow L_R', e_R \leftrightarrow e_L', \quad Q_L \leftrightarrow Q_R', \quad u_R \leftrightarrow u_L', d_R \leftrightarrow d_L'. \end{aligned}$$

One of the advantages of this model, as we discussed above, is that there are natural candidates of non-baryonic dark matter in addition to restore parity [6]. It was shown [6] that this model does not contradict with the astrophysical and cosmological observations.

In the following we focus on the Higgs sector of this mirror model. There are two Higgs fields ϕ_1 and ϕ_2 , which are doublets under $SU(2)$ and $SU(2)'$ respectively. One assumes that the Higgs potential is invariant under the discrete symmetry $\phi_1 \rightarrow \phi_2$ to keep the parity in a broader sense. The Higgs potential is very simply given by

$$\begin{aligned} V(\phi_1, \phi_2) &= -\mu^2 \left(\phi_1^\dagger \phi_1 + \phi_2^\dagger \phi_2 \right) + \lambda \left(\phi_1^\dagger \phi_1 + \phi_2^\dagger \phi_2 \right)^2 \\ &+ \eta \phi_1^\dagger \phi_1 \phi_2^\dagger \phi_2. \end{aligned} \quad (2)$$

After electro-weak symmetry breaking, the Higgs fields can be written as

$$\phi_i = \left(\frac{1}{\sqrt{2}} (v_i + H_i + \chi_i) \right), \quad (3)$$

where $\varphi_i^\dagger, \chi_i$ are Goldstone bosons, which will be absorbed by corresponding gauge fields. The vacuum may not be invariant under Z_2 transformation although the

Higgs potential is invariant under this discrete transformation. In fact there are two ways of spontaneous symmetry breaking, depending on the choice of the sign of η [15]. We will discuss these two cases separately below.

1. $\eta < 0$.

In this case, vacuum is invariant under transformation $\phi_1 \leftrightarrow \phi_2$.

$$v^2 = v_1^2 = v_2^2 = \frac{2\mu^2}{4\lambda + \eta}. \quad (4)$$

We define Higgs boson mass eigenstates as H, h (in this paper we assume H is heavier than h),

$$H_1 = \frac{1}{\sqrt{2}}(H + h) \quad (5)$$

$$H_2 = \frac{1}{\sqrt{2}}(H - h). \quad (6)$$

The Higgs boson mass can be expressed as

$$m_H^2 = (4\lambda + \eta)v^2 \quad (7)$$

$$m_h^2 = -\eta v^2. \quad (8)$$

Obviously there must be $\eta < 0$, which is coincide with the condition of minimizing Higgs potential.

2. $\eta > 0$.

For this case, if we require the minimum of Higgs potential is stable, then

$$v_1^2 = \frac{\mu^2}{\lambda}, v_2^2 = 0. \quad (9)$$

The Higgs boson masses are

$$m_h^2 = \frac{\mu^2}{2}, m_H^2 = \frac{\eta v_1^2}{8} \quad (10)$$

It seems that all the mirror particles must be massless. However mirror particle can obtain tiny mass through mirror QCD condensation[15, 17], but we don't discuss this case further in this paper.

In this paper we only consider the first case, i.e. the vacuum is invariant under Z_2 parity transformation. It should be noted that the Z_2 discrete symmetry of Higgs potential may be broken by small term. Such term will lead to very different effect [16].

In order to study the phenomenology of this model, we choose the Higgs boson masses m_H, m_h as inputs, so

$$\lambda = \frac{m_H^2 + m_h^2}{4v^2}, \eta = -\frac{m_h^2}{v^2}. \quad (11)$$

The Lagrangian of triple interaction of Higgs bosons, which we are interested in, is given by

$$\mathcal{L}_{int} = \omega H h^2, \quad (12)$$

$$\omega = \frac{\sqrt{2} m_H^2 + 2m_h^2}{4v} \quad (13)$$

The other triple and quadruple Higgs interactions can be inferred from the potential easily which are not shown here.

Thus, if kinematically allowed, $H \rightarrow hh$ decay width can be expressed as

$$\Gamma(H \rightarrow hh) = \frac{\omega^2}{8\pi m_H^2} \sqrt{1 - \frac{4m_h^2}{m_H^2}}. \quad (14)$$

From Eqs. 13 and 14, we can see that the large decay width is possible for the favorable parameters.

III. CONSTRAINTS FROM ELECTRO-WEAK PRECISION OBSERVABLE

Current electro-weak precision observable (EWPO) can give constraints on the physics beyond the SM. A widely used set of parameters are S, T and U [18]. Such parametrization assumes that the new physics contributions arise only from propagators of the electro-weak gauge bosons, namely the oblique corrections [18]. The mirror model belongs to this case.

We calculate the Higgs bosons contributions to S, T parameters in the mirror model. Here we do not consider U parameter because U is very small in general.

We give our results as following

$$S = \frac{1}{2}[S_{SM}(m_h) + S_{SM}(m_H)] - S_{SM}(m_{ref}) \quad (15)$$

$$T = \frac{1}{2}[T_{SM}(m_h) + T_{SM}(m_H)] - T_{SM}(m_{ref}) \quad (16)$$

where [19]

$$\begin{aligned} S_{SM}(m) &= \frac{1}{\pi} \left[\frac{3}{8} \frac{m^2}{m_Z^2} - \frac{1}{12} \frac{m^4}{m_Z^4} + \frac{m^2}{m_Z^2} \log \frac{m^2}{m_Z^2} \right. \\ &\times \left(\frac{3m_Z^2 - m^2}{4m_Z^2} + \frac{1}{24} \frac{m^4}{m_Z^4} + \frac{3m_Z^2}{4(m_Z^2 - m^2)} \right) \\ &\left. + \left(1 - \frac{1}{3} \frac{m^2}{m_Z^2} + \frac{1}{12} \frac{m^4}{m_Z^4} \right) \frac{m}{m_Z^2} f \right] \end{aligned} \quad (17)$$

with

$$f = \begin{cases} \sqrt{4m_Z^2 - m^2} \arctan \sqrt{\frac{4m_Z^2 - m^2}{m^2}} \\ \text{if } m < 2m_Z \\ \sqrt{m^2 - 4m_Z^2} \log \frac{2m_Z}{m + \sqrt{m^2 - m_Z^2}} \\ \text{if } m > 2m_Z \end{cases}, \quad (18)$$

and

$$T_{SM}(m) = \frac{3}{16\pi} \frac{1}{s_W^2 c_W^2} \left[\frac{m^2}{m_Z^2 - m^2} \log \frac{m^2}{m_Z^2} - \frac{c_W^2 m^2}{c_W^2 m_Z^2 - m^2} \log \frac{m^2}{c_W^2 m_Z^2} \right] \quad (19)$$

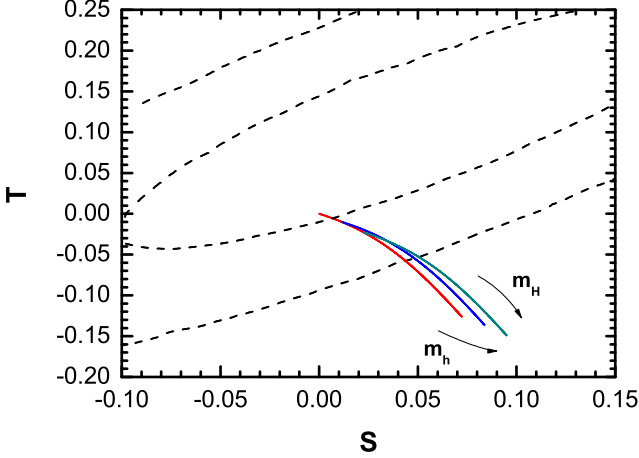


FIG. 1: The ellipses indicate the regions in the S, T plane which are allowed by EWPO at 1σ (68%) and 2σ (95%) level respectively [20]. Three curves represent three different m_h at 115, 150 and 200 GeV, and m_H increases from 100 ~ 1000 GeV for each curve.

The numerical results of S and T are shown in Fig. 1. From the figure we can see that EWPO has already constrained the Higgs boson masses severely, similar to the SM. For example, if we fix $m_h = 115\text{GeV}$, the 95% CL upper limit of m_H can approach about 300 GeV. In the following numerical evaluation we choose $m_H = 260\text{GeV}$ and $m_h = 115\text{GeV}$ as our benchmark point, except indicated otherwise.

IV. HIGGS BOSON PHENOMENOLOGY

In order to discuss the Higgs boson phenomenology, it is convenient to divide parameters into: (1) $m_H < 2m_h$, namely H can't decay into a pair of h , and (2) $m_H > 2m_h$.

A. Higgs Boson Decay

As mentioned above, each Higgs boson (h and H) is the mixture state of the ordinary and the mirror Higgs fields. As a consequence, each Higgs boson can decay into both ordinary and mirror fermions, gauge bosons if kinematically allowed. In the specific model discussed in this paper, the branching ratio of the lighter Higgs boson h decaying into SM particles (fermions and gauge bosons)

will be modified as (taking bottom quark as an example)

$$\begin{aligned} Br(h \rightarrow b\bar{b}) &= \frac{\Gamma(h \rightarrow b\bar{b})}{\Gamma(h \rightarrow SM) + \Gamma(h \rightarrow Mirror)} \\ &= \frac{1}{2} Br(h_{SM} \rightarrow b\bar{b}), \end{aligned} \quad (20)$$

where $Br(h_{SM} \rightarrow b\bar{b})$ represents branching ratio of the SM Higgs boson decaying into bottom quarks. The expressions for h decaying into mirror particles are the same with those into ordinary SM particles.

The branching ratios of the heavier Higgs boson H are the same with those of h in Eq. 20 for the case (1), in which $H \rightarrow hh$ is kinematically forbidden. Note that we omit here the tiny three body decay of $H \rightarrow hh^* \rightarrow h f \bar{f}$. However for case (2), $H \rightarrow hh$ is allowed. The formula for the branching ratios of $Br(H \rightarrow hh)$ and $Br(H \rightarrow b\bar{b})$ are

$$\begin{aligned} & \frac{Br(H \rightarrow hh) [Br(H \rightarrow b\bar{b})]}{\Gamma(H \rightarrow SM) + \Gamma(H \rightarrow Mirror) + \Gamma(H \rightarrow hh)} \\ &= \frac{\Gamma(H \rightarrow hh) [\Gamma(H \rightarrow b\bar{b})]}{2\Gamma(H \rightarrow SM) + \Gamma(H \rightarrow hh)}. \end{aligned} \quad (21)$$

In Fig. 2, we show the branching ratios of H to $t\bar{t}$, W^+W^- , ZZ and hh as a function of m_H with $m_h = 115$ GeV. From the figure it is obvious the branching ratio of $H \rightarrow hh$ is larger than that of $Br(H \rightarrow ZZ)$ and sizable once it is kinematically allowed. Note that Hhh coupling is proportional to $m_H^2 + 2m_h^2$.

If H can decay into a pair of Z boson, it is not difficult to find such kind Higgs boson via the 'golden' mode with 4 charged lepton final states. However in the mirror model the branching ratio of $H \rightarrow ZZ$ can be lower than 20%, much higher luminosity than that of SM is needed to find such kind of the Higgs boson.

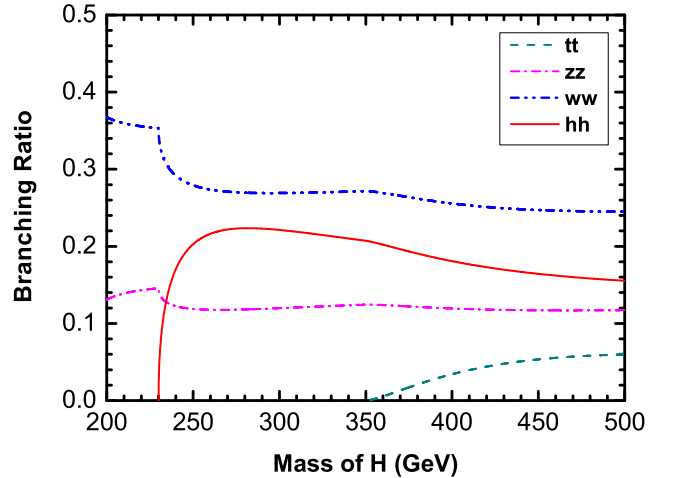


FIG. 2: Branching ratios of H as a function of m_H , where $m_h = 115\text{GeV}$.

B. Higgs Boson Production

In the specific model we discussed in this paper, the production rate of single Higgs boson h (H) at colliders is only half of that in the SM. Similar to the SM, the main production channels at the LHC are $gg \rightarrow h(H)$ or $qq' \rightarrow h(H)V$ with $V = (W, Z)$. For the light Higgs boson, another important production processes are $gg, qq \rightarrow t\bar{t}h(H)$. If the mass difference of two Higgs bosons h and H is larger than that of detector mass resolution, we may discover two separate mass peaks out of continuum backgrounds with the much higher luminosity compared to that in the SM. Note that the branching ratio of h to the SM particles, as shown in the last subsection, is only half of that of SM. Similarly more luminosity is needed in order to measure the properties of the Higgs bosons.

In order to investigate the triple and quadruple couplings among Higgs bosons, it is necessary to study the pair production of Higgs bosons. In the mirror model, there are three combinations of the Higgs boson pair, i.e. hh , hH and HH . For case (1) it is hard to investigate such signatures at the LHC due to the low production rate, similar to that of the SM.

For case (2), hh production can be enhanced due to the s-channel H resonance. Thus the Higgs boson pair hh production rate can be much larger than that of case (1). Such enhancement provides one promising way to study the mirror model. We will focus on this scenario in the following subsection.

In Fig. 3 and Fig. 4 we show the cross sections for the single H and hh pair production as a function of m_H . From the figures it is obvious that the hh pair production can easily reach several hundred of femtobarns.

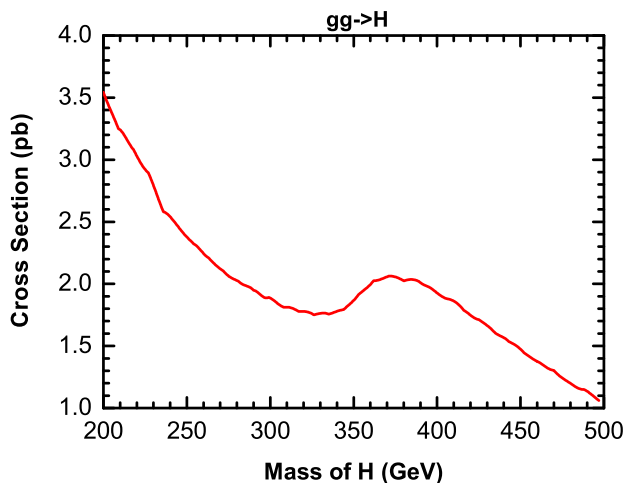


FIG. 3: Cross sections of $gg \rightarrow H$ as a function of m_H at the LHC.

In literature there are extensive investigations on processes $H \rightarrow hh \rightarrow$ light quarks and/or leptons and/or $\gamma\gamma$ [21, 22, 23, 24, 25], where h represents light scalar or pseudoscalar. If h is heavy enough, the channel of $H \rightarrow hh \rightarrow 4W$ would open [26]. However such scenario

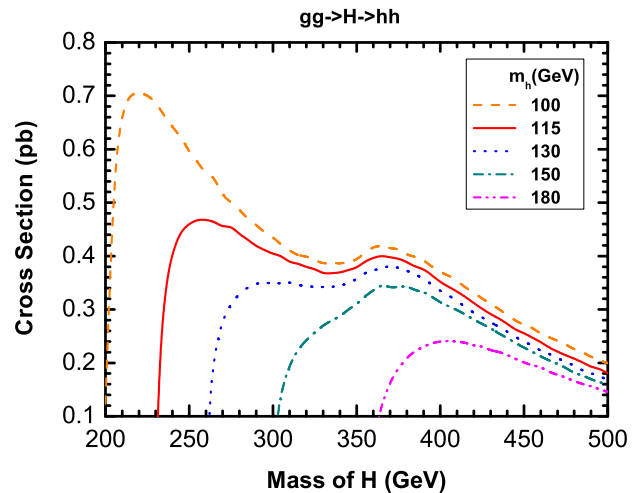


FIG. 4: Cross sections [in pb] of $gg \rightarrow H \rightarrow hh$ as a function of m_H at the LHC, where $m_h = 100, 115, 130, 150$ and 180 GeV from top to bottom.

is not favored by the precision data, as shown in section III. In the mirror model, in order to maintain the signal rate, we require that one lighter Higgs boson h decay into $b\bar{b}$, and the other lighter Higgs boson has many decay modes. In this paper we focus on two modes: (1) h decays into mirror particles which has the largest branching ratio of 50%; and (2) h decays into $b\bar{b}$ which has the second largest branching ratio, larger than that of l^+l^- or $\gamma\gamma$ etc.

It should be mentioned the other possible channel, namely $qq' \rightarrow V + H \rightarrow \ell + 4b$, which can also be utilized to study $H \rightarrow hh$ [22]. As shown in Ref. [22], for light Higgs boson with the mass around 100 GeV, this process may provide a clean signature out of the backgrounds. But for $m_H = 260$ GeV, there are large background from $gg \rightarrow t\bar{t}$ with $t\bar{t} \rightarrow \ell + 2b + 2j$, and from light quark jets with two of them misidentifying as b jets.

V. DETAIL SIMULATIONS

In this section, we will simulate the signals and backgrounds for the process $gg \rightarrow H \rightarrow hh$ choosing $m_H = 260$ GeV and $m_h = 115$ GeV as the typical parameters. We utilize Madgraph/MadEvent 4.1.27 [27] and Pythia 6.4.11 [28] to simulate the backgrounds and signals at the LHC with the CTEQ5L PDF set. We ignore initial and final QCD and QED radiation corrections. For the sake of simplicity, we assume the b -tagging efficiency of 50% and mis-tagging efficiencies for c , g and light quarks of 10%, 1% and 1%, respectively [24].

A. $gg \rightarrow H \rightarrow hh \rightarrow b\bar{b} + \text{Mirror Particles}$

In the mirror model, the largest branching ratio of h is the decay into mirror particles. Because the mirror

particles appear as the missing energy at colliders, such decaying h can't be directly reconstructed via its decay products, i.e. h decays invisibly. In order to investigate $H \rightarrow hh$, we require that the other h must decay into bottom quarks, which is the largest *visible* decay mode for our choice of m_h .

As pointed out in the Introduction, the invisible Higgs boson has been extensively investigated in literature [11, 12, 13]. In this section, we investigate the observability of invisible Higgs boson at the LHC, via the process

$$p p \rightarrow g g \rightarrow H \rightarrow h(\rightarrow b^+ b^-) + h_{inv}, \quad (22)$$

where one h decays into bottom quarks and the other decays invisibly. As it was known [11], one of the disadvantages of this $b\bar{b} + \cancel{P}_T$ signal is that $b\bar{b}$ final states are not easy to be reconstructed completely.

The most important irreducible background arises from $Zb\bar{b}$ production

$$p p \rightarrow Z(\rightarrow \nu\bar{\nu})b\bar{b}, \quad (23)$$

where Z decays into neutrinos. Moreover QCD multi-jet production, such as $p p \rightarrow Z(\rightarrow \nu\bar{\nu})jj$, are also the sources of the large backgrounds. In this paper we require two b-tagged jets in order to suppress these backgrounds. Other backgrounds can arise from ZZ , WZ , $Wb\bar{b}$, single top and $t\bar{t}$ production [11].

We utilize MadEvent [27] to simulate all backgrounds, and apply the basic kinematical cuts as following

$$P_T(j_1), P_T(j_2) > 20 \text{ GeV}, 15 \text{ GeV} \quad (24)$$

$$|\eta_j| < 2 \quad (25)$$

$$\Delta R(jj) > 0.4 \quad (26)$$

$$m_{jj} > 10 \text{ GeV}, \quad (27)$$

where P_T denotes the transverse momentum of jet, η denotes the pseudo-rapidity, and $\Delta R = \sqrt{(\Delta\eta)^2 + (\Delta\phi)^2}$ with ϕ the azimuthal angle.

In the following we discuss how to suppress the backgrounds from $Wb\bar{b}$, WZ , single top with $t \rightarrow bW$ and $t\bar{t} \rightarrow bW\bar{b}W$. For these backgrounds, the final state charge leptons or jets from W escape from the detection. We suppress these contributions by vetoing events from W decay with follow cuts

$$P_T(j) > 15 \text{ GeV}, |\eta(j)| < 2.0 \quad (28)$$

$$P_T(l^\pm) > 10 \text{ GeV}, |\eta(l^\pm)| < 2.5 \quad (29)$$

The numerical results after imposing cuts Eqs. 24-29 are shown in Tab. I. It is obvious that the dominant backgrounds come from the $Zb\bar{b}$ production.

The signals and backgrounds for $b\bar{b} + \cancel{P}_T$ as a function of \cancel{P}_T are shown in Fig. 5, where we reconstruct \cancel{P}_T from $b\bar{b}$. We can see that the signals peak within the $40 \text{ GeV} < \cancel{P}_T < 80 \text{ GeV}$ window, while the backgrounds are flat. In order to suppress the backgrounds, we impose the further cuts as following

$$|m_{jj} - m_h| < 15 \text{ GeV} \quad (30)$$

$$40 \text{ GeV} < \cancel{P}_T < 80 \text{ GeV}. \quad (31)$$

Channel	$Zb\bar{b}$	$Zb\bar{c}$	Zbj	$Zc\bar{c}$	Zcj	Zjj
$\sigma(\text{pb})$	3.250	0.011	0.107	0.001	0.027	0.063
Channel	ZZ	$W^-b\bar{b}$	W^-Z	$t\bar{b}$	$t\bar{t}$	
$\sigma(\text{pb})$	0.072	0.417	0.032	0.017	0.346	

TABLE I: The cross sections (in pb) of backgrounds for $b\bar{b} + \cancel{P}_T$ after basic kinematical cuts Eqs. 24-29 and tagging efficiencies where $j = u, \bar{u}, d, \bar{d}, s, \bar{s}, g$.

It is natural to impose the cut of Eq. 30 because we can extract the approximate mass information of Higgs boson via other process, for example $gg \rightarrow h \rightarrow \gamma\gamma$.

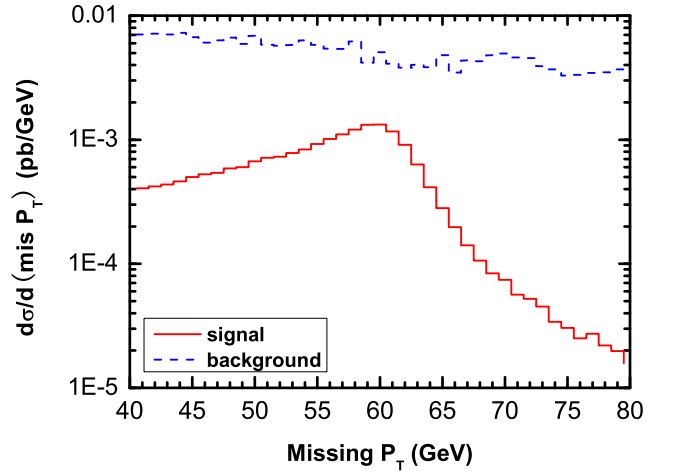


FIG. 5: The distributions of the signals and backgrounds for $b\bar{b} + \cancel{P}_T$ as a function of \cancel{P}_T after applying cuts Eqs 24-29 and tagging efficiencies.

We show the signals and backgrounds as the function of $|\eta_{j_1} - \eta_{j_2}|$ after imposing all above cuts Eqs. 24-31 in Fig. 6. The figure shows that signals decrease quicker than that of backgrounds for $|\eta_{j_1} - \eta_{j_2}| < 2$, which provides a possible way to suppress backgrounds further. We require

$$|\eta_{j_1} - \eta_{j_2}| < 1.5, \quad (32)$$

and this cut would improve significance of the signals by a factor of 1.2, as shown explicitly in Tab. II.

From the Fig. 6, we can see that the backgrounds are still much larger than those of the signals. The dominant backgrounds come from the irreducible $Zb\bar{b}$ production. We would like to explore another additional potentially useful methods to reduce the this huge background, similar to the case in Ref. [12].

In order to suppress the largest $Zb\bar{b}$ background, we can utilize the precise measurement of $Z(\rightarrow \mu^+\mu^-)b\bar{b}$, similar to that in Ref. [12]. The reason is that the backgrounds $Z(\rightarrow \nu\bar{\nu})b\bar{b}$ have similar kinematics and distributions to those of $Z(\rightarrow \mu^+\mu^-)b\bar{b}$ production. We can obtain improved (reduced) background $Zb\bar{b}$ as following

$$\sigma_{bkg}^{Zb\bar{b}, imp} = \sigma_{bkg}^{Zb\bar{b}} - R \times \sigma_{b\bar{b}\mu^+\mu^-}. \quad (33)$$

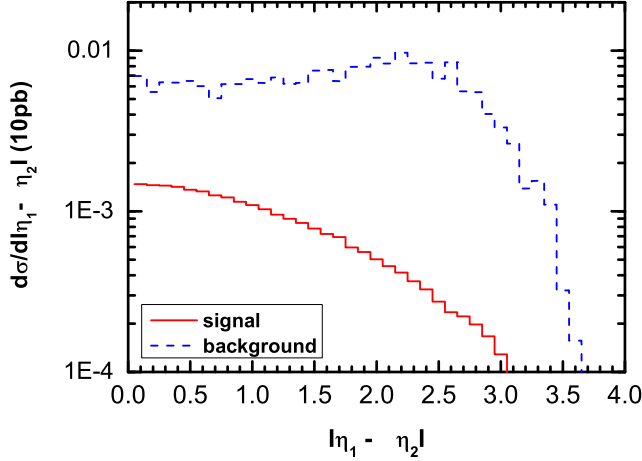


FIG. 6: The distributions of the signals and backgrounds for $b\bar{b} + \cancel{p}_T$ as a function of $|\eta_{j1} - \eta_{j2}|$ after imposing cuts Eqs. 24-31 and tagging efficiencies.

In Eq. 33, $\sigma_{b\bar{b}\mu^+\mu^-}$ is the cross section for $Z(\rightarrow \mu^+\mu^-)b\bar{b}$ production which adopts the same kinematical cuts for $Z(\rightarrow \nu\bar{\nu})b\bar{b}$. R is a ratio which is defined as

$$R = \frac{\sum_i Br(Z \rightarrow \nu_i \bar{\nu}_i)}{Br(Z \rightarrow \mu^+ \mu^-)}, \quad (34)$$

and in our case $R = 5.94$ [12]. Note that $\sigma_{bkg}^{Zb\bar{b}, imp} \approx 0$ if we can measure all final states $b\bar{b}\mu^+\mu^-$ in any kinematical region.

However we are aware of the difficulties of this method. For example, in order to combine two measurements, at least we must deal with two different systematics, and fully understand the detectors etc. Detail study on this method is obviously beyond the scope of this paper, and we show here only the rough estimation.

Cuts	$s(fb)$	$b(fb)$	S/B	$S/\sqrt{B_1}$	$S/\sqrt{B_2}$
basic cuts	26.6	4948	0.0054	1.19	2.07
$ m_{jj} - m_h < 30\text{GeV}$	26.6	1133	0.023	2.50	4.32
$ m_{jj} - m_h < 15\text{GeV}$	26.6	492	0.054	3.79	6.56
$20 < \cancel{p}_T < 120\text{GeV}$	25.0	401	0.062	3.94	6.83
$40 < \cancel{p}_T < 80\text{GeV}$	19.4	202	0.096	4.33	7.49
$ \eta_{j1} - \eta_{j2} < 1.5$	15.2	95	0.16	4.93	8.54
improved backg	15.2	18	0.83	11.4	19.8

TABLE II: The effects on the cross sections of signal (s) and background (b), ratio of signal and background events S/B , $S/\sqrt{B_1}$ and $S/\sqrt{B_2}$, by imposing cuts of Eqs.24-33 step by step, are summarized. Here $m_H = 260$ GeV and $m_h = 115$ GeV. The significance $S/\sqrt{B_1}$ is for the luminosity of $10fb^{-1}$ and $S/\sqrt{B_2}$ is for the luminosity of $30fb^{-1}$. All the numbers shown here are after tagging efficiencies.

All numerical results after imposing cuts step by step for Eqs. 24-33 are summarized in Tab. II. From Tab. II, we can see that at the LHC, the channel $H \rightarrow hh \rightarrow b\bar{b} + \cancel{p}_T$ can provide about $5\sigma(11\sigma)$ significance observation

with only $10fb^{-1}$ after applying the cuts Eqs. 24-30 and suitable \cancel{p}_T window, without (with) further suppressing the $Zb\bar{b}$ backgrounds using Eq. 33. In other words, it is not difficult to detect $H \rightarrow hh \rightarrow b\bar{b} + \text{mirror particles}$ at the LHC. To see this explicitly, we give the luminosity (Tab. III) which is required to achieve 5σ observation for different m_H and m_h .

	$m_h = 100\text{GeV}$	$m_h = 115\text{GeV}$	$m_h = 130\text{GeV}$
$m_H = 250$ GeV	8.2(40,80)	8.3(10,60)	--
$m_H = 300$ GeV	9.0(80,130)	9.6(60,110)	17.5(40,80)
$m_H = 350$ GeV	5.5(100,150)	6.6(90,140)	11.6(80,120)

TABLE III: The integrated luminosity [in fb^{-1}], which is required to observe $H \rightarrow hh \rightarrow b\bar{b} + \cancel{p}_T$ with 5σ significance at the LHC, for several sets of m_H and m_h . The numbers in bracket are mass window of \cancel{p}_T . Note the Eq. 33 is not applied.

B. $gg \rightarrow H \rightarrow hh \rightarrow 4b$

In Ref. [24], the authors studied the general $4b$ signal in extended SUSY models (with $p_T^j > 15$ GeV) at Tevatron. They concluded that for the SM case $gg \rightarrow h$ has not enough rate, an order of magnitude smaller, for the light SM Higgs boson with mass less than 150 GeV. However if the signal is sufficiently enhanced, $4b$ signal may be detectable. As we have shown, the hh production rate can be greatly enhanced once $H \rightarrow hh$ is allowed. In this section we use the same strategy to investigate $4b$ signals and backgrounds as those in Ref. [24].

Most of the backgrounds for $gg \rightarrow H \rightarrow hh \rightarrow 4b$ are due to the contributions from large QCD multijet production. We adopt basic kinematical cuts as Eqs.(24)~(27). Moreover we require at least tagging three b -jets to reduce the huge backgrounds. The backgrounds drop from $0.106mb$ to $3.21nb$. In order to suppress the backgrounds further, we require $|m_H - m_{4j}| < 20$ GeV and $|m_h - m_{jj}| < 15$ GeV.

In Fig. 7 we show the signals and backgrounds as a function of invariant mass of four jets. It is obvious that the backgrounds are much larger, around three orders of the magnitude, than those of the signals. The main reason is that the gluon-gluon luminosity drops very quickly with the increment of the m_H .

VI. DISCUSSIONS AND CONCLUSIONS

The Higgs sector may play an important role in detecting the mirror particles, which can be the candidates of the dark matter and appear as missing energy in the detectors at the LHC. In this paper we worked out the Higgs boson spectrum and the Higgs couplings for the symmetric vacuum, namely $v_1 = v_2 = v$, in the mirror

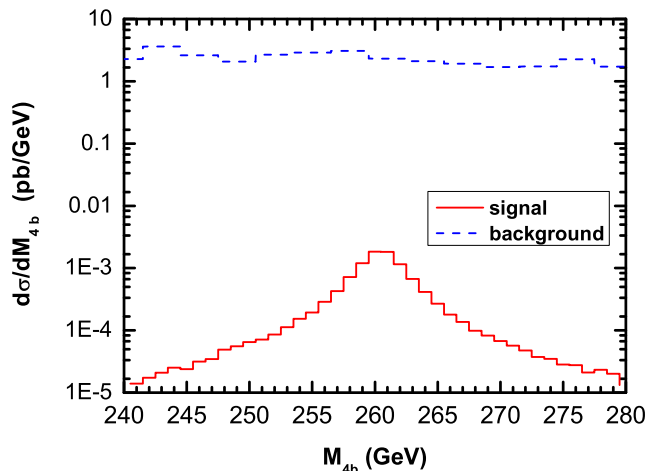


FIG. 7: The distributions of the signals and backgrounds for bbb as a function of invariant mass for $4b$ after applying cuts (see text) and tagging efficiencies.

model [14], and investigated the constraints from electroweak precision observable (EWPO). Our study showed that the EWPO has already constrained the Higgs boson sector severely. We then investigated the Higgs boson phenomenology, and focused on the scenario that the heavier Higgs boson H can decay into a pair of lighter Higgs boson h .

As the generic feature in the mirror model, Higgs boson can decay invisibly. The invisible Higgs boson can be detected via the processes [12, 13] of $q\bar{q} \rightarrow ZH$, weak gauge boson fusion $VV \rightarrow H$ or $gg \rightarrow t\bar{t}H$ etc. In this paper we proposed to study the invisible decay of the Higgs boson via pair production of them, in which one

Higgs boson decays into bottom quarks and the other decays invisibly. Our detail simulation for signals and backgrounds showed that the observation of signal can reach 5σ significance for $m_H = 260$ GeV and $m_h = 115$ GeV with $10fb^{-1}$ integrated luminosity at the LHC. It should be emphasized that our conclusion also applies to other models in which the Higgs boson pair production cross section is $O(100)$ femtobarns and the branching ratio of invisible decay is sizable. Moreover the possible method to further suppress dominant $Zb\bar{b}$ background was discussed.

We also simulated the signals and backgrounds for $H \rightarrow hh \rightarrow 4b$ at the LHC. Our results showed that it is very difficult to isolate the signals from huge QCD continuum backgrounds.

In the mirror model, the heavier Higgs boson H may not decay into a pair of lighter Higgs boson h . For such case, it is hard to study the triple Higgs couplings of hhH . In fact even $H \rightarrow hh$ is allowed, the other triple Higgs couplings such as hhh and HHH are very difficult to measure at the LHC. Therefore ILC is the necessary next facility of investigating Higgs triple, even quadruple couplings.

VII. ACKNOWLEDGEMENTS

SHZ thanks Prof. K.T. Chao and Prof. Y.P. Kuang for drawing the attention to the issue of parity restoration. This work was supported in part by the Natural Sciences Foundation of China (No. 90403004, 10775001 and 10635030), the trans-century fund and the key grant project (No. 305001) of Chinese Ministry of Education.

-
- [1] J. C. Pati and A. Salam, Phys. Rev. D **10**, 275 (1974).
 - [2] R. N. Mohapatra and J. C. Pati, Phys. Rev. D **11**, 566 (1975).
 - [3] T. D. Lee and C. N. Yang, Phys. Rev. **104**, 254 (1956).
 - [4] L. B. Okun, arXiv:hep-ph/0606202.
 - [5] R. F. G. Wyse and G. Gilmore, arXiv:astro-ph/0708.1492.
 - [6] For the recent review to see, R. Foot, arXiv:hep-ph/0706.2694.
 - [7] R. Foot, R. R. Volkas, Phys. Rev. D **52**, 6595 (1995).
 - [8] B. Holdom, Phys. Lett. B **187**, 65 (1986).
 - [9] E. D. Carlson, S. L. Glashow, Phys. Lett. B **272**, 67 (1991).
 - [10] S. N. Gninenko, Phys. Lett. B **326**, 317 (1994); R. Foot and S. N. Gninenko, Phys. Lett. B **480**, 171 (2000); A. Badertscher, P. Crivelli, W. Fetscher, U. Gendotti, S. Gninenko, V. Postoev, A. Rubbia, V. Samoylenko and D. Sillou, Phys. Rev. D **75**, 032004 (2007).
 - [11] S. P. Martin and J. D. Wells, Phys. Rev. D **60**, 035006 (1999).
 - [12] S. H. Zhu, Eur. Phys. J. C **47**, 833 (2006).
 - [13] D. Choudhury and D. P. Roy, Phys. Lett. B **322**, 368 (1994); S. G. Frederiksen, N. Johnson, G. L. Kane and J. Reid, Phys. Rev. D **50** (1994) 4244; H. Davoudiasl, T. Han and H. E. Logan, Phys. Rev. D **71**, 115007 (2005); R. M. Godbole, M. Guchait, K. Mazumdar, S. Moretti and D. P. Roy, Phys. Lett. B **571**, 184 (2003); O. J. P. Eboli and D. Zeppenfeld, Phys. Lett. B **495**, 147 (2000).
 - [14] R. Foot, H. Lew and R. R. Volkas, Phys. Lett. B **272**, 67 (1991).
 - [15] R. Foot, H. Lew, R. R. Volkas, JHEP **032**, 0007 (2000).
 - [16] R. Barbieri, T. Gregoire and L. J. Hall, arXiv:hep-ph/0509242.
 - [17] R. Foot and H. Lew, arXiv:hep-ph/9411390.
 - [18] M. E. Peskin and T. Takeuchi, Phys. Rev. Lett **65**, 964 (1990); *ibid*, Phys. Rev. D **46**, 1 (1992).
 - [19] For example to see, J. R. Forshaw, D. A. Ross and B. E. White, JHEP **0110**, 007 (2001).
 - [20] R. Barbieri, arXiv:hep-ph/0706.0684.
 - [21] P. F. Yin and S. h. Zhu, arXiv:hep-ph/0611270.
 - [22] K. Cheung, J. Song and Q. S. Yan, Phys. Rev. Lett **99**, 031801 (2007).
 - [23] M. Bowen, Y. Cui and J. D. Wells, JHEP **0703**, 036 (2007).
 - [24] T. Stelzer, S. Wiesenfeldt and S. Willenbrock, Phys. Rev.

- D **75**, 077701 (2007).
- [25] For many other $H \rightarrow \eta\eta$ studies, see the Ref. [4] of [24].
- [26] U. Baur, T. Plehn, and D. L. Rainwater, Phys. Rev. D **67**, 033003 (2003).
- [27] T. Stelzer and W. F. Long, Comput. Phys. Commun **81**, 357 (1994); F. Maltoni and T. Stelzer, JHEP **0302**, 027 (2003).
- [28] T. Sjostrand, S. Mrenna and P. Skands, JHEP **0605**, 026 (2006).
- [27] T. Stelzer and W. F. Long, Comput. Phys. Commun **81**,